EUROFUSION WPPFC-PR(16) 14724

G Riva et al.

Pull-off force measurements for tungsten dust adhered to tungsten surfaces

Preprint of Paper to be submitted for publication in
22nd International Conference on Plasma Surface Interactions
in Controlled Fusion Devices (22nd PSI)

This work has been carried out within the framework of the EUROfusion Consortium and has received funding from the Euratom research and training programme 2014-2018 under grant agreement No 633053. The views and opinions expressed herein do not necessarily reflect those of the European Commission.

Adhesion measurements for tungsten dust deposited on tungsten surfaces

G. Riva,[1] P. Tolias,[2] S. Ratynskaia,[2] G. Daminelli,[1] R. Donde,[1] M. De Angeli,[3] E. Vassallo[3] and M. Pedroni[3]

[1] *Institute of Condensed Matter Chemistry and Energy Technologies - Consiglio Nazionale delle Ricerche, via Cozzi 53, 20125 Milan, Italy*
[2] *Space and Plasma Physics - KTH Royal Institute of Technology, Teknikringen 31, 10044 Stockholm, Sweden*
[3] *Istituto di Fisica del Plasma - Consiglio Nazionale delle Ricerche, via Cozzi 53, 20125 Milan, Italy*

Abstract

The first experimental determination of the pull-off force for tungsten dust adhered to tungsten surfaces is reported. Dust deposition is conducted with gas dynamics methods in a manner that mimics sticking as it occurs in the tokamak environment. Adhesion measurements are carried out with the electrostatic detachment method. The adhesion strength is systematically characterized for spherical micron dust of different sizes and planar surfaces of varying roughness. The experimental pull-off force is nearly two orders of magnitude smaller than the predictions of contact mechanics models, but in satisfactory agreement with the Van der Waals formula. A theoretical interpretation is provided that invokes the effects of nanometer-scale surface roughness for stiff materials such as tungsten.

1. Introduction

It has been recently recognized that adhesion plays a pivotal role in various tokamak issues concerning dust [1, 2]. For instance, upon dust-wall mechanical impacts, adhesive work is responsible for a significant part of the overall dissipation of the normal dust velocity component [3, 4, 5]. Moreover, during loss-of-vacuum accidents, dust mobilization occurs when hydrodynamic forces overcome the net adhesive force [6]. Furthermore, under steady state or transient plasma conditions, dust remobilization takes place when plasma-induced forces exceed the net adhesive force, also known as pull-off force [7, 8]. Finally, the quantification of the pull-off force is an essential step towards the development of *in situ* dust removal techniques suitable for future fusion devices such as ITER [9, 10]. Nevertheless, to date, there have been no pull-off force measurements for reactor relevant materials.

Experimental techniques that characterize the strength of dust-surface adhesion are generally based on exerting a well-known force in a controlled environment until mobilization is observed [11]. The colloidal probe method of atomic force microscopy (AFM) measures the cantilever deflection at the detachment instant, which after careful calibration can be converted into a spring force [12, 13, 14]. The centrifuge detachment method employs the centrifugal force arising from a rapidly rotating surface [15]. The electrostatic detachment method employs the electrostatic force resulting from the interaction between an externally imposed electric field and the contact charge it induces on the conducting dust surface [16]. The colloidal probe method is the most accurate, but it involves single grain measurements and thus acquiring statistics can be very time-consuming [11]. On the contrary, the centrifuge and electrostatic detachment methods are less precise but involve multiple simultaneous measurements.

In this work we report on the first pull-off force measurements for tungsten dust adhered to tungsten surfaces carried out with the electrostatic detachment method. The dust grains were adhered to the W surfaces in a manner that realistically mimics dust sticking as it occurs in tokamaks [7]. The strength of adhesion has been characterized for different micrometer-range sizes of W dust deposited on W surfaces of varying roughness. Comparison with theory revealed that contact mechanics models overestimate the pull-off force by nearly two orders of magnitude, whereas microscopic Van der Waals models provide pull-off force values close to the experimental. It is argued that this is the consequence of nano-scale roughness; for stiff metals such as tungsten, even the smallest departure from atomic smoothness can remarkably reduce the surface energy due to the extremely short range of metallic bonding.

2. Theoretical aspects

Different expressions for the sphere-plane pull-off force can be derived by two somewhat complementary theoretical descriptions of the contact of solid bodies. The microscopic description is applicable to non-deformable solids and considers the overall effect of Lennard-Jones type interactions, neglecting chemical bonding. On the other hand, the macroscopic description is applicable to deformable solids and only considers the effect of short-range forces of chemical bonding nature in the contact zone. Clearly, the macroscopic description is more appropriate for atomically smooth, *i.e.* zero roughness perfectly planar or spherical, solids. In what follows, we shall provide a brief presentation of the microscopic and macroscopic descriptions for smooth materials and discuss the multifaceted effects of surface roughness separately.

In microscopic descriptions of the contact, the pull-off force is calculated from simple balance considerations. When chemical bonding is negligible, the pull-off force needs to counteract the overall interaction between the instantaneously induced and / or permanent multipoles inside the bodies, which constitutes the attractive Van der Waals interaction. For a spherical dust grain of radius $R_{\rm d}$ in the proximity of a planar surface, the Van der Waals force is given by [17]

$$F_{\rm po}^{\rm VdW} = \frac{A}{6z_0^2}\, R_{\rm d}\,, \tag{1}$$

where $z_0 (\ll R_{\rm d})$ is the distance of closest approach between the two surfaces and A is known as the Hamaker constant. When considering the contact of two identical smooth metals, z_0 can be assumed equal to the lattice parameter that is 3.16 Å for W [18]. The Hamaker constant is generally calculated on the basis of the Lifshitz continuum theory. For identical metals embedded in vacuum, neglecting the temperature-dependent entropic term and assuming a collisionless free electron permittivity $\epsilon(\omega) = 1 - \omega_{\rm pe}^2/\omega^2$ we acquire $A \simeq [3/(16\sqrt{2})]\hbar\omega_{\rm pe}$ [19]. The plasma frequency of W is $\omega_{\rm pe} \sim 7 \times 10^{15}\,{\rm rad/sec}$ [20] leading to the estimate $A \sim 10^{-19}\,{\rm J}$, which is close to the value recommended in the literature $A \simeq 4 \times 10^{-19}\,{\rm J}$ [17]. Note that the Van der Waals force is not important for smooth metals in intimate contact, since the interaction due to metallic bonding (owing to the sharing of the delocalized valence electrons) is dominant [21].

In macroscopic descriptions of the contact, the pull-off force is calculated by the contact mechanics approach [22]. The interaction strength is indirectly considered via the work of adhesion (per unit area) defined by $\Delta\gamma = \gamma_1 + \gamma_2 - \Gamma$, where γ_i denotes the surface energy, Γ the interface energy and in the case of identical metals $\Gamma \simeq 0$, $\Delta\gamma \simeq 2\gamma$ [23]. The surface energy is externally adopted either from first principle calculations [24] or from experiments [25], for tungsten $\gamma = 4.36\,{\rm J/m^2}$. When ignoring plasticity, established contact mechanics models, in spite of their different assumptions and validity ranges, lead to a pull-off force of the form [26]

$$F_{\rm po}^{\rm CMA} = \xi_{\rm a}\pi\Delta\gamma R_{\rm d}\,, \tag{2}$$

with $3/2 \leq \xi_{\rm a} \leq 2$ a dimensionless coefficient [27]. The Johnson-Kendall-Roberts (JKR) theory leads to the coefficient $\xi_{\rm a} = 3/2$ [28], whereas the Derjaguin-Muller-Toporov (DMT) theory leads to the coefficient $\xi_{\rm a} = 2$ [29]. The aforementioned adopted value of γ incorporates metallic bonding in an automatic manner and the above expression is appropriate for metals in intimate contact. We point out that metallic forces are extremely short range and they can be considered to be effectively zero already for distances larger than 1 nm [30]. Consequently, as metallic dust approaches a smooth metal surface, the interaction is initially of the Van der Waals type and switches to the metallic type, which is stronger by orders of magnitude, only for distances close to the lattice parameter [30].

Surface roughness is known to significantly modify the pull-off force. Its presence alters many aspects of the contact and its effects can be categorized in the following manner: **(I)** Pure geometrical effects that occur due to changes in the local curvature of the bodies and their point-point separation. These have been considered in microscopic descriptions by decomposing the overall interaction into a contact term with the spherical asperity and a non-contact term with the underlying plane, where the statistically varying asperity parameters are expressed with the aid of measurable roughness characteristics [31, 32]. **(II)** Deformation effects that occur due to the existence of different asperity heights, which lead to a competition between the compressive elastic forces exerted by the higher asperities and the adhesive forces exerted by the lower asperities. The former tend to detach the contacting bodies, effectively reducing the pull-off force [23]. Such effects have been considered in macroscopic descriptions by applying the JKR theory to individual asperity micro-contacts, assuming a Gaussian distribution for their height with respect to the average plane and summing up the force contributions [33]. They can be expected to be important for stiff materials with large elastic moduli. In general, refractory metals are characterized by a large Young's modulus and tungsten, in particular, has one of the largest values, $E \simeq 410\,{\rm GPa}$ in room temperature. **(III)** Bond switching effects that occur when the asperity dimensions are larger than or comparable to the range of interatomic forces. In this case, some parts of the bodies interact via weak van der Waals forces and other parts of the bodies form strong chemical bonds.

Even mirror-polished tungsten surfaces are characterized by root-mean square measures of roughness $R_{\rm q}$ that significantly exceed the range of the metallic bond. Plasma exposed surfaces and tokamak-born dust can certainly be expected to have roughness $R_{\rm q} \gg 1\,{\rm nm}$. Therefore, we can safely assume that interaction via metallic bonding is limited in a very small fraction of the contact area and that it is further effectively reduced by deformation effects. This suggests that interaction via van der Waals forces is dominant. Finally, for simplicity and as a crude approximation, we can neglect pure geometrical effects and employ Eq.(1) for the pull-off force.

3. Experimental aspects

The electrostatic detachment of micron-size metallic dust from metallic surfaces requires the application of strong fields that may lead to dielectric breakdown. Since low pressures can significantly increase the breakdown voltage, the experiments were conducted into a vacuum chamber with a pressure < 0.05Pa. This also eliminates humidity, known to affect pull-off force measurements. The electrostatic field was generated by two parallel electrodes, see Fig.1 for a schematic representation.

Electrostatic detachment. The configuration can be idealized as consisting of a rigid spherical conductor in con-

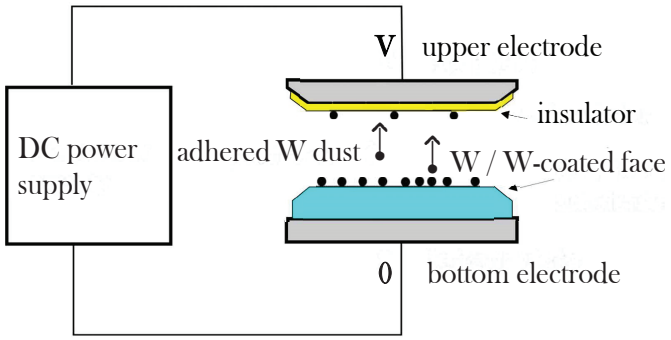

Figure 1: Simple schematic of the high-voltage system and the electrode composition for the pull-off force measurements.

tact with a grounded plane in the presence of a uniform normal electrostatic field. For this geometry, the Laplace equation for the potential can be analytically solved with the aid of degenerate bi-spherical coordinates. In cgs units, the contact charge of the sphere is given by the expression $Q_{\rm d} = -\zeta(2)R_{\rm d}^2 E$ and the repelling normal electrostatic force acting on the sphere by $F_{\rm e} = [(1/6) + \zeta(3)]R_{\rm d}^2 E^2$, where $\zeta(.)$ denotes Riemann's zeta function [34]. The expression can be rewritten as

$$F_{\rm e} = kE^2 R_{\rm d}^2 \ \ (\mu{\rm N})\,, \qquad (3)$$

with $k = 1.52 \times 10^{-4} (\mu{\rm N} \cdot {\rm mm}^2)/({\rm kV}^2 \mu{\rm m}^2)$, the field expressed in kV/mm and the radius in μm. Owing to $F_{\rm e} \propto E^2 R_{\rm d}^2$ and $F_{\rm po} \propto R_{\rm d}$, force balance leads to $E \propto 1/\sqrt{R_{\rm d}}$ for the electrostatic field. Hence, small dust grains require larger mobilizing fields, which are not always possible to generate due to dielectric breakdown.

Electrode preparation. The upper face of the bottom electrode should consist of pure tungsten. Due to metal-working difficulties, it was not possible to manufacture full W electrodes of the appropriate geometry and alternative solutions had to be sought. **(i)** Four electrodes were constructed by coating the upper face of different metal substrates (brass, copper, aluminum) with a W layer. The film was deposited by rf-diode argon plasma sputtering. A thin titanium inter-layer (300 nm) was deposited to increase the film adhesion. In order to minimize well-known stress phenomena [35], a multi-layer strategy was adopted, featuring alternating growth at low (8×10^{-3} mbar) and high (3×10^{-2} mbar) gas pressures. The overall layer depth was $\sim 3.5\,\mu$m, thick enough to ensure that adhesive forces stem exclusively from W-W interactions. **(ii)** Three electrodes were constructed by inserting already available small bulk W cylinders into hollow brass electrodes of the desired dimensions. The roughness characteristics were controlled by implementing sandpapers of different grades. Meanwhile, the bottom face of the upper electrode was spray coated with an acrylic layer of $\sim 40\,\mu$m thickness. The presence of the insulating film was necessary to restrict the amount of mobilized dust grains that re-deposited on the bottom electrode, after impact and charge exchange with the upper electrode [16]. The acrylic coating nearly eliminated this problem.

Dust preparation & deposition. Spherical W dust with a nominal size distribution $5 - 25\,\mu$m (diameter) was supplied by TEKNA Advanced Materials. Sub-populations with narrower size distributions were generated by a meshing method utilizing ultrasonic cells. The size distributions of the three sub-populations relevant for these experiments are illustrated in Fig.2. Their most probable diameters are 5, 9 and 16 μm. The W dust was deposited on the upper face of the bottom electrode, whose W surface was cleaned with a total evaporation dry deoxidizer and compressed air. The deposition was carried out with gas dynamics methods in a manner that realistically mimics dust sticking as it occurs in the tokamak environment. Adhesion was achieved by controlling the dust impact speed below the sticking threshold. See Ref.[7] for a detailed description of the device and the operation principle. In order to reduce the number of agglomerates, the mediated adhesion technique [7] was employed with 4 mm diameter plastic (delrin) spheres of 2 m/s impact speed acting as dust carriers.

Experimental procedure. After the dust deposition, the bottom electrode was mounted into the vacuum chamber. A pre-selected high voltage difference was applied to the electrodes and maintained. The mobilization activity was monitored by detecting the attenuation of a laser diode beam, focused above the dust spots. Irrespective of the information provided by this optical system, the electric field was cancelled after 6 min and the chamber was opened. The bottom electrode was dismounted and images of the dust spots were taken by a camera applied to an optical microscope, typically with a 200 magnification factor. The bottom electrode was mounted again and a slightly higher electric field was supplied. The same procedure was repeated until all dust grains had been removed or until the breakdown limit was reached. The electric field steps were not constant, they generally ranged from 1 to 5 kV/mm.

4. Experimental results

The dust spot images corresponding to adjacent electrostatic field strengths are overlaid with the aid of software and the number of grains mobilized during each exposure is determined. Two datasets are built: one only considering mobilization of isolated dust, one considering mobilization of all grains in direct contact with the substrate including small clusters provided that they do not contain grains elevated with respect to the substrate surface (the latter generally identifiable as they appear unfocused). In this work, only results concerning isolated dust are reported, as the two datasets provide similar qualitative information.

By image superposition, we can acquire the immobile dust fraction as a function of the applied electrostatic field. A characteristic example is provided in Fig.3. Ideally, this graph should have the form of a step function with the discontinuity located at the unique electric field solution of the force balance equation $F_{\rm e}(E, R_{\rm d}) = F_{\rm po}(R_{\rm d})$. The

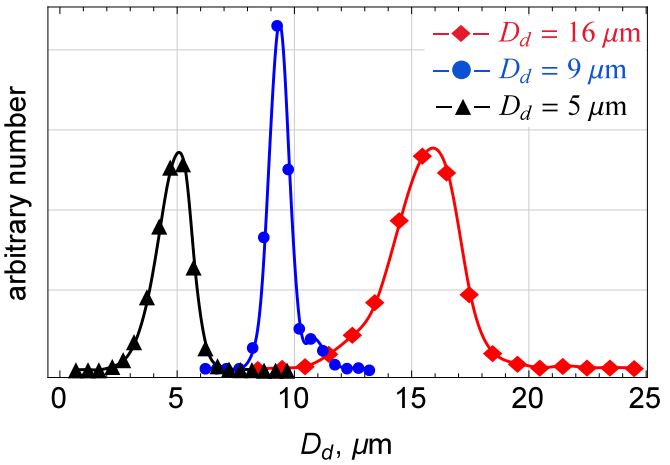

Figure 2: Size distributions for the three meshed spherical W dust sub-populations. The horizontal axis corresponds to the dust diameter $D_{\rm d}$. The most probable diameters are 5, 9 and 16 μm. The size distributions are approximately symmetric, hence the average diameters are nearly equal to the most probable diameters.

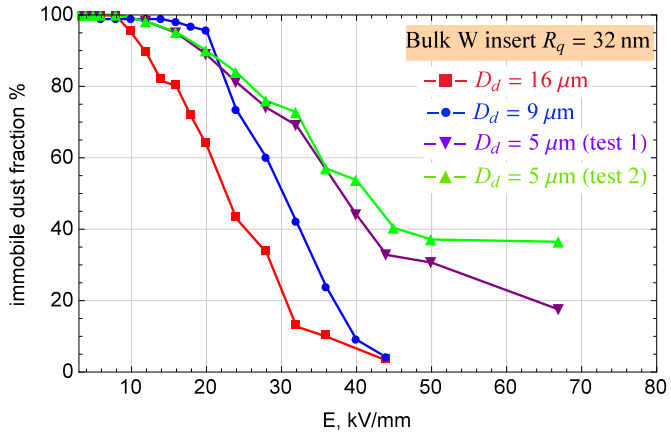

Figure 3: Characteristic experimental output featuring the fraction of isolated dust grains that remain immobile as a function of the applied electrostatic field strength. Results for a bulk tungsten substrate of $R_{\rm q}$ = 32 nm and all three W dust sub-populations (corresponding to the last four rows of Table 1).

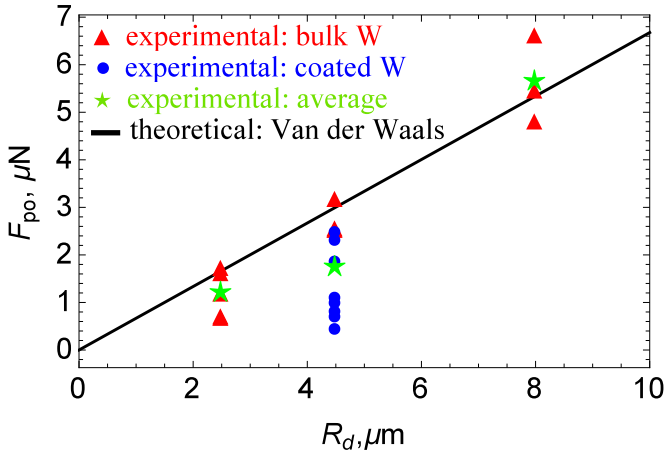

Figure 4: The strength of adhesion for spherical W dust of varying size deposited on planar W substrates of varying roughness. The experimental weighted average pull-off force for each set of measurements, the set averaged pull-off force and the theoretical pull-off force due to Van der Waals interactions as a function of the dust radius.

sources of the deviations from the step function are the following; (i) Unavoidable randomness due to the smallness of the contact area combined with the presence of roughness. A small number of asperities can fit within any contact area, which implies that the geometrical characteristics of the asperities cannot be represented by their averages. (ii) Uncertainties in the dust radii due to the spread of the size distributions. (iii) Uncertainties in the electrostatic force due to the fact that the applied voltage difference increases in discrete steps. (iv) Small uncertainties in the contact area due to plasticity effects during the impact. In deposition with the mediated adhesion technique, the dust impact speed is generally smaller than the dust carrier speed. Thus, plastic deformation follows a distribution. (v) Small uncertainties in the mobilizing force, due to electrostatic interactions between the contact-charged dust grains.

Due to the aforementioned uncertainties, the experimental pull-off force will be statistically distributed. We denote the total number of isolated dust grains by N, the total number of measurements by M and the most probable dust size by $R_{\rm d,p}$. During the $i-$th measurement, let N_i be the number of detached dust grains and $F_{{\rm e},i} = kR_{\rm d,p}^2 E_i^2$ the electrostatic force. The weighted average pull-off force will be given by

$$\bar{F}_{\rm po} = \sum_{i=1}^{M} \left[\left(\frac{N_i}{N} \right) kR_{\rm d,p}^2 E_i^2 \right] / \sum_{i=1}^{M} \left(\frac{N_i}{N} \right) . \qquad (4)$$

In case the maximum electrostatic field achieved before dielectric breakdown sufficed to mobilize all dust grains, the denominator is equal to unity. In case some dust grains remained immobile, the denominator is smaller than unity and increases the value of the weighted sum. Therefore, the inclusion of the denominator compensates for the lack of strong field measurements. The weighted average is an accurate representation of the experimental pull-off force, provided that there is a small immobile dust fraction remaining after breakdown. This criterion is not satisfied in experiments carried out with the 5 μm dust subpopulation. The experimental results are summarized in Table 1.

Averaging over the different measurement sets, we can obtain a unique $\bar{\bar{F}}_{\rm po}(R_{\rm d})$ value that represents the experimental data for each size regardless of the substrate roughness, see Fig.4 (the data points represented by green stars). For $R_{\rm d} = 2.5\mu$m; we acquire the value 1.20 μN, the Van der Waals result is 1.67 μN, the JKR theory yields 102.7 μN and the DMT theory yields 137 μN. For $R_{\rm d} = 4.5\mu$m; we acquire 1.73 μN, the Van der Waals result is 3.00 μN, the JKR theory yields 184.9 μN and the DMT theory yields 246.6 μN. For $R_{\rm d} = 8\mu$m; we acquire 5.64 μN, the Van der

Table 1: Summary of pull-off force measurements by electrostatic detachment for spherical W dust adhered to W surfaces. Total of 19 sets of measurements carried out with 7 different substrates and 3 different dust sub-populations.

Substrate composition	Substrate roughness R_q (nm)	Most probable diameter (μm)	Number of isolated dust grains	F_e range $20\% - 80\%$ mobilization (μN)	immobile dust fraction (%)	maximum electric field (kV/mm)	average pull-off $\bar{F}_{po}$ (μN)
W coated brass	619	9	85	0.11-2.08	13	36	0.71
(3.6 μm thickness)		9	148	0.20-2.08	6	36	1.11
W coated brass	76	9	20	0.05-0.79	10	18	0.45
(3.6 μm thickness)		9	92	0.25-1.49	8	36	0.82
W coated Cu	33	9	243	1.36-3.77	17	36	2.49
(3.5 μm thickness)		9	271	0.31-1.36	0.4	36	1.00
W coated Al	20	9	61	1.11-2.24	10	36	1.87
(3.5 μm thickness)		9	351	1.36-2.77	3	36	2.32
bulk W insert in	104	16	42	2.81-5.60	7	40	4.82
hollow brass		9	194	1.11-5.69	18	44	2.54
electrode (polished)		5	290	0.31-3.42	29	60	0.72
bulk W insert	100	16	216	2.49-7.63	3	40	5.47
in hollow		9	516	1.11-3.15	4	45	2.57
brass electrode		5	930	1.52-2.87	60	55	1.74
(polished)		5	430	0.50-2.87	65	55	0.69
bulk W insert	32	16	140	2.49-9.35	4	44	6.63
in hollow		9	661	1.63-4.21	4	50	3.19
brass electrode		5	1078	0.59-3.89	17	67	1.63
(polished)		5	1093	0.64-4.26	36	67	1.20

Waals result is 5.34 μN, the JKR theory yields 328.7 μN and the DMT theory yields 438.3 μN. Therefore, the contact mechanics approach values are approximately two orders of magnitude larger than the measurements, while the van der Waals values lie very close to the measurements. Heuristically, it can be stated that the effective surface energy of the real system is much smaller than the thermodynamic surface energy. In fact, by combining Eqs.(1,2) with $\xi_a = 3/2$ for the JKR theory we can define the effective surface energy $\gamma_{eff} = A/(18\pi z_0^2)$. This results to $\gamma_{eff} \simeq 0.071\,\mathrm{J/m^2}$, which is smaller than $\gamma_{th} = 4.36\,\mathrm{J/m^2}$ by a factor of 60. It is important to point out that other experimental studies have also indicated that $\gamma_{eff} \ll \gamma_{th}$ [13]. A microscopic mechanism that leads to this difference has been discussed in section 2.

5. Summary and future work

The pull-off force for micron-size tungsten dust adhered to planar tungsten surfaces has been measured with the electrostatic detachment method. The experimental results exhibit a satisfactory agreement with the Van der Waals force expression for a distance of closest approach equal to the lattice parameter 3.16 Å and the recommended value of the Hamaker constant 4×10^{-19} J. The results also reveal that the pull-off force is approximately two orders of magnitude less than the value predicted by contact mechanics approaches (JKR and DMT theory), as expected by a qualitative analysis of the contact of rough stiff materials.

The latter observation has important implications for dust remobilization under steady state or transient plasma conditions [7, 8]. Recent systematic cross-machine investigations of dust remobilization have revealed that adhered micron-size W grains can rarely exhibit an intense remobilization activity (even exceeding 50%) [7]. In the aforementioned work, JKR theory was employed in order to demonstrate that adhesive forces are at least two orders of magnitude stronger than plasma-induced forces. Consequently, in light of the experimental results, a number of possible mechanisms were sought to explain the observed remobilization. One of the proposed mechanisms involved decrease of the pull-off force from its nominal JKR value by orders of magnitude owing to omnipresent nano-scale roughness. The present measurements clearly support this mechanism. More important, they constitute necessary input for theoretical models of dust remobilization.

In the present work, owing to the inherent uncertainties of the electrostatic detachment method and the lack of surface roughness measurements for the dust grains, it was not possible to quantify the effect of varying rms roughness on the pull-off force. Future work will focus on more precise pull-off force measurements with the AFM colloidal probe method, which should also allow for an investigation of the roughness dependence.

Acknowledgments

This work has been carried out within the framework of the EUROfusion Consortium and has received funding from the Euratom research and training programme 2014-2018 under grant agreement No 633053. Work performed under EUROfusion WP PFC. The views and opinions expressed herein do not necessarily reflect those of the European Commission.

[1] S. Ratynskaia, C. Castaldo, H. Bergsåker and D. Rudakov, *Plasma Phys. Control. Fusion* **53** (2011) 074009.
[2] S. I. Krasheninnikov, R. D. Smirnov and D. L. Rudakov, *Plasma Phys. Control. Fusion* **53** (2011) 083001.
[3] S. Ratynskaia, L. Vignitchouk, P. Tolias, I. Bykov *et al.*, *Nucl. Fusion* **53** (2013) 123002.
[4] L. Vignitchouk, P. Tolias and S. Ratynskaia, *Plasma Phys. Control. Fusion* **56** (2014) 095005.
[5] A. Shalpegin, F. Brochard, S. Ratynskaia, P. Tolias *et al.*, *Nucl. Fusion* **55** (2015) 112001.
[6] S. Peillon, A. Roynette, C. Grisolia and F. Gensdarmes, *Fusion Eng. Des.* **89** (2014) 2789.
[7] P. Tolias, S. Ratynskaia, M. De Angeli, G. De Temmerman *et al.*, *Plasma Phys. Control. Fusion* **58** (2016) 025009.
[8] S. Ratynskaia, P. Tolias, I. Bykov, D. Rudakov *et al.*, *Nucl. Fusion* (2016) (in press).
[9] C.-H. Choi, A. Tesini, R. Subramanian, A. Rolfe *et al.*, *Fusion Eng. Des.* **98-99** (2015) 1448.
[10] E. Veshchev, G. Vayakis, G. De Temmerman, K. Ebisawa *et al.*, *Conceptual design of a dust monitor diagnostic for ITER*, Proceedings of the 1st EPS conference on Plasma Diagnostics, Frascati, Italy, 2015
[11] H. Mizes, M. Ott, E. Eklund and D. Hays, *Colloids Surf. A* **165** (2000) 11.
[12] D. M. Schaefer, M. Carpenter, B. Gady, R. Reifenberger *et al.*, *J. Adhesion Sci. Technol.* **9** (1995) 1049.
[13] L.-O. Heim, J. Blum, M. Preuss and H.-J. Butt, *Phys. Rev. Lett.* **83** (1999) 3328.
[14] J. Drelich and K. L. Mittal, *Atomic force microscopy in adhesion studies*, VSP, Leiden-Boston, 2005.
[15] D. F. St. John and D. J. Montgomery, *J. Appl. Phys.* **42** (1971) 663.
[16] D. W. Cooper and H. L. Wolfe, *Aerosol Sci. Technol.* **12** (1990) 508.
[17] J. N. Israelachvili, *Intermolecular and surface forces*, Academic Press, New York, 2011.
[18] D. A. Papaconstantopoulos, *Handbook of the band structure of elemental solids*, Springer, New York, 2015.
[19] F. L. Leite, C. C. Bueno, A. L. Da Róz, E. C. Ziemath and O. N. Oliveira, *Int. J. Mol. Sci.* **13** (2012) 12773.
[20] A. P. Lenham and D. M. Treherne, *J. Opt. Soc. Am.* **56** (1966) 1076.
[21] B. Bhushan, *J. Vac. Sci. Technol. B* **21** (2003) 2262.
[22] K. L. Johnson, *Contact Mechanics*, Cambridge University Press, Cambridge, 1985.
[23] D. Tabor, *J. Colloid Interface Sci.* **58** (1977) 2.
[24] L. Vitos, A. V. Ruban, H. L. Skriver and J. Kollár, *Surf. Sci.* **411** (1998) 186.
[25] G. Czack, G. Kirschstein, W. Kurtz and F. Stein, *Tungsten: Gmelin Handbook of Inorganic and Organometallic Chemistry vol A4*, Springer, Berlin, 1993.
[26] B. Cappella and G. Dietler, *Surf. Sci. Rep.* **34** (1999) 1.
[27] D. Maugis, *J. Colloid Interface Sci.* **150** (1992) 243.
[28] K. L. Johnson, K. Kendall and A. D. Roberts, *Proc. R. Soc. A* **324** (1971) 301.
[29] B. Derjaguin, V. M. Muller and Y. P. Toporov, *J. Colloid Interface Sci.* **53** (1975) 314.
[30] L.-H. Lee, *Fundamentals of adhesion*, Springer Science, New York, 1991.
[31] H. Rumpf, *Particle Technology*, Chapman & Hall, London, 1990.
[32] Y. I. Rabinovich, J. J. Adler, A. Ata, R. K. Singh and B. M. Moudgil, *J. Colloid Interface Sci.* **232** (2000) 10.
[33] K. N. G. Fuller and D. Tabor, *Proc. R. Soc. A* **345** (1975) 327.
[34] N. N. Lebedev and I. P. Skalskaya, *Sov. Phys. Tech. Phys.* **7** (1962) 268.
[35] T. Karabacak, C. R. Picu, J. J. Senkevich, G.-C. Wang and T.-M. Lu, *J. Appl. Phys.* **96** (2004) 5740.